Photon production from collisions of 100–350-keV positive ions with CO, CF_4, and CH_4

Eric J. Freeman,* Elisabeth L. Bryan,† and Michael N. Monce
Department of Physics and Astronomy, Connecticut College, New London, Connecticut 06320
(Received 12 August 1991; revised manuscript received 9 March 1992)

Various photon emissions from collisions of H^+, H_2^+, and He^+ in the 100–350-keV energy range with targets of CO, CF_4, and CH_4 were studied. The wavelength range of the investigation ran from 2000 to 7000 Å. Photon-emission cross sections were measured for all significant features. The cross-section data were compared to the Bethe-Born theory through the use of Fano plots. The results show that the theory could be applicable in the case of the CO target, but is probably not applicable to the tetrahedral molecular targets as the emissions are from dissociated atoms.

PACS number(s): 34.70.+e, 34.50.Gb, 82.30.Fi

I. INTRODUCTION

In general, studies of collisional processes serve two functions. Foremost, they provide the practical data necessary to model phenomena in such diverse fields as stellar and planetary atmospheres, radiation damage in solids, surface bombardment, thermonuclear fusion, track studies in nuclear emulsions, health physics, and plasma physics [1,2]. More fundamentally, however, the information extracted from collisional processes provide basic information about the particles involved and the causes and effects of interaction. In this paper we examine the photon emission from excitations produced in collisions of positive ions with molecular targets CO, CF_4, and CH_4.

Surprisingly little work has been done examining the collision-produced photon emission from carbon monoxide even though it is a major component of comets [3,4] and thus subject to solar wind bombardment. Also, as a relatively simple diatomic molecule, carbon monoxide provides the opportunity to extend studies begun on targets such as H_2 and N_2. The authors found one previous paper by Poulizac, Desesquelles, and Dufay [5], published in 1969, that examined photon-emission spectra produced by 30–600-keV protons on CO. Those data, however, were not corrected for beam attenuation or for polarization sensitivity of the optical system; also, a McLeod gauge was used for target-gas pressure measurement, but no correction was made for thermal transpiration. With improvements implemented in this study, the error in measured cross sections decreases from 50% in their study to 20% in the present one. We also extend the data by the use of He^+ and H_2^+ beams.

For charge-transfer and ionization cross sections of positive ions on CO the studies have been more numerous. Afrosimov *et al.* looked at the interaction of 5–50-keV protons and hydrogen atoms with CO molecules [6]. Sataka, Yagishita, and Nakai measured the charge-changing cross sections in collisions of He and He^+ with various molecules, including CO [7]. Most recently, Shah and Gilbody [8] examined ionization and electron capture from H^+ and He^{2+} on CO at velocity ranges of 10–98 keV/u for H^+ and 6.7–65 keV/u for He^{2+}. Rudd and co-workers have produced two studies of positive-ion impact on various gases including CO [2,9]. The first examined ionization by 5–4000-keV protons and electron capture by 5–150-keV protons, while the second examined ionization by 10–2000-keV He^+ ions and electron capture and loss by 5–350-keV He^+ ions.

Providing an interesting contrast with regard to the photon-emission processes involved, we also examine CF_4 (Freon-14) and CH_4. Freon is of importance to atmospheric chemistry as it contributes to ozone depletion. Recent concern about global warming has led to studies that have shown both of these gases to be considerable contributors to the greenhouse effect [10]. New developments in the dry etching of computer components, which makes use of plasmas containing CF_4, have piqued interest in the poorly understood collision processes involving this molecule. Besides being a pollutant in the earth's atmosphere, methane is of particular interest in the study of Jupiter because its upper atmosphere contains traces of methane [11].

Recent experiments involving the excitation of CF_4 have consisted mainly of electron impact [12–16], photoelectron studies [17,18], and dissociation cross sections [19]. Sasaki, Kuen, and Howorka [20] have reported excitation cross sections in collisions of eight positive ions in the energy range of 1–1800 eV with CF_4. Aarts [21] has studied vacuum ultraviolet and UV emissions from CF_4 under impact of 1–25-keV He^+, Ne^+, and H^+. As far as the authors are aware, there is currently no data available on collisionally induced emissions from ion impact on CF_4 in the energy range of 100–350 keV.

Existing studies of photon emission from target excitation of CH_4 have focused mainly on electron [12–16,22] and proton impact [23]. Geddes, Yousif, and Gilbody [24] have studied both target and projectile emission in collisions of 10–100 keV H, H^+, H_2^+, and H_3^+ with CH_4. Previous work from this laboratory investigated Balmer-α emissions from CH_4 under impact of 100–350-keV He^+ [25].

II. EXPERIMENTAL PROCEDURE

A. General description

The details of the experimental apparatus and procedure have been previously published [25–27]. Briefly, the ion beams were produced by a Van de Graaff accelerator and momentum was analyzed by a 90° magnet. The beam entered a differentially pumped target chamber after being collimated to approximately 2–3 mm. After passing through a target-gas cell, the beam was collected by a Faraday cup. Photons emitted at 90° to the beam direction were analyzed by a monochromator and detected by a photomultiplier tube. The resolution of the monochromator was generally greater than the line width, so all emitted photons from a particular line were counted. The photon detection system was calibrated with respect to its absolute sensitivity by standard techniques, and corrections were made for polarization and anisotropy effects [28] through the use of a polarizing filter whose axis of polarization could be set parallel or perpendicular to the beam line. The target-gas pressure was 3 mTorr, which was measured by a capacitance manometer. Temperature was measured by a thermistor. Typical ion-beam currents were on the order of 0.3 μA at the Faraday cup.

Signals from the capacitance manometer, the monochromator, the thermistor, the Faraday cup, and the photomultiplier tube were fed into a data-acquisition system, which performed analog-to-digital conversion of these voltage signals and channeled them to a computer. These data were then assimilated by programs written in ASYST 3.0 to produce cross sections corrected for beam current, temperature, gas pressure, and optical system sensitivity. To find the value for the beam attenuation, the beam current from the collimator and the Faraday cup was converted into a voltage signal and read by the computer for both 0 and 3 mTorr.

As a check of the calibration of the optical system, the emission cross sections for the 3914-Å band and the 4278-Å band of N_2^+ were measured using a proton beam. Hoffman, Lockwood, and Miller have made a very precise determination of these cross sections for use as a standard [29]. Our measurements of these cross sections agreed with Hoffman's measurements within 3%.

The estimated error due to experimental systematics in all the absolute photon-emission cross sections reported here is 20%. Approximately three-quarters of the error is due to measurement of the sensitivity of the optical system, while one-quarter is due to statistical uncertainty and error from measurements of the target pressure, temperature, and beam current.

B. Beam neutralization

A major correction to the data involved accounting for beam neutralization in cross-section measurement. The attenuation in the beam was calculated by measuring the beam current on both the Faraday cup and the collimator with no gas in the target chamber. Target gas was then introduced, and a second measurement of both collimator and cup currents was taken to produce a neutralization ratio. The measurement of the collimator current was necessary in order to take into account that the overall beam intensity may change during the attenuation measurement. This attenuation value was used to correct the integrated Faraday cup current taken during the cross-section measurement. The ratio of collimator to cup current is determined by the focus conditions of the accelerator. The maximum percent attenuation of the ion beam was 71%, 56%, and 57% for a 100-keV He^+ beam on the CF_4, CO, and CH_4 targets, respectively. The H_2^+ and the proton beams exhibited a maximum attenuation of about 26% with a CO target, and 37% with the Freon-14 target. All values for the attenuation decreased in an approximately $1/E$ manner, where E is the projectile energy.

Such large attenuation percentages indicate that we must correct for the production of neutral species in the beam, especially in the case of the lower-energy helium beams. Beam neutralization can occur at any point along the beam path, but will be most prevalent within the target-gas cell.

If we have a beam of charged particles entering a gas cell of length l, some of those particles will be neutralized as they pass through the gas cell. At the energies we are working at, this comes about primarily from charge capture. We will ignore outscattering. Then the expression for the photon emission over a distance dx within the cell will be

$$dJ=\sigma_0 N I_{b0} dx+\sigma_+ N I_{b+} dx \ , \tag{1}$$

where N is the target density, I_{b0} is the beam consisting of neutral species, σ_0 is the photon-emission cross section for the neutral species, I_{b+} is the beam consisting of charged particles, and σ_+ is the photon-emission cross section for the charged particles.

Just before entering the target cell there will be a total beam I_b such that at any point in the gas cell $I_b=I_{b0}+I_{b+}$. The charged-particle portion of the beam will be depleted by

$$\frac{dI_{b+}}{dx}=-\sigma_c N I_{b+} \tag{2}$$

or

$$I_{b+}=I_b e^{-\sigma_c N x} \ , \tag{3}$$

where σ_c is the cross section for charge capture. The photon emission over a length dx in terms of the initial beam impinging on the cell is then

$$dJ=\sigma_0 N(I_b-I_b e^{-\sigma_c N x})dx+\sigma_+ N I_b e^{-\sigma_c N x} dx \ , \tag{4}$$

so the total photon-emission rate will be

$$J=\sigma_0 N I_b \int_0^l (1-e^{-\sigma_c N x})dx+\sigma_+ N I_b \int_0^l e^{-\sigma_c N x} dx \ . \tag{5}$$

For the pressures we are working at, we can use the expansion for the exponentials in the integrals

$$e^{-\sigma_c N x}\approx 1-\sigma_c N x+\frac{\sigma_c^2 N^2 x^2}{2} \ . \tag{6}$$

Making this substitution and performing the integrals yields the following result:

$$J=\sigma_0 N I_b l\left[\sigma_c N\frac{l}{2}-\frac{\sigma_c^2 N^2 l^2}{6}\right]+\sigma_+ N I_b l\left[1-\sigma_c N\frac{l}{2}+\frac{\sigma_c^2 N^2 l^2}{6}\right]. \quad (7)$$

From this last equation we can obtain an expression for the photon-emission cross section

$$\frac{J}{N I_b l}=\sigma_+\left[1-\sigma_c N\frac{l}{2}+\frac{\sigma_c^2 N^2 l^3}{6}\right]+\sigma_0\left[\sigma_c N\frac{l}{2}-\frac{\sigma_c^2 N^2 l^3}{6}\right]. \quad (8)$$

If there were no neutralization occurring, then the first bracket term would be one and the second bracket term would be zero. To get a value for the correction needed, we calculated the values of the brackets in the above equation using the capture cross sections for He^+ on CO and CH_4 from Rudd *et al.* [9]. The worst case occurs for 100-keV He^+, where Eq. (8) yields a 14% correction. This correction value decreases rapidly as the capture cross section decreases with increasing beam energy.

For the case of the CF_4 target there appear to be no published cross sections for capture. In order to get a reasonable estimate for the capture cross section from the CH_4 target, we used the capture cross sections for the methane target as an estimate for the same cross section for the CF_4 target. They are similar in structure and size so this should be a reasonable approximation.

In studying these processes in this energy range from these targets, we are unaware of any data on the excitation by the neutral helium portion of the beam. The recent work of Geddes, Yousif, and Gilbody [24] has shown that in the case of a methane target, the cross section for excitation by the H^0 beam is about 67% greater than the proton beam at 100 keV. Using that data, we then estimated a value for σ_0 in Eq. (8). We justify this on the basis of the Bethe-Born theory, in which the emission cross section is dependent on the charge of the projectile for equivelocity particles. In other words, in Eq. (8) we substitute for σ_0 a constant (from Geddes data) times σ_+ for the appropriate value of keV/u.

Finally, in applying the results of Eq. (8) in correcting the data we must be careful with regard to the value used for I_b. Generally, this is the unattenuated beam entering the target-gas cell. However, there is leakage of the target-gas upstream from the gas cell, which will cause beam neutralization prior to entering the gas cell. Thus, our value of I_b as obtained from the initial attenuation measurements could be in error. We have made an estimate of this effect. By knowing the pressure differential between the gas cell and the ambient pressure (3 mTorr and 10^{-6} Torr), and the length of the beam collimator, we calculated the number of target molecules encountered by the beam prior to the gas cell through the use of the diffusion equation. We then used the known cross sections for capture to estimate the amount of the beam that is neutralized. The result is about 3% for the He^+ beam at 100 keV and correspondingly less for higher energies and for the other two beams.

The procedure used in making the above outlined corrections is as follows: The integrated beam current as measured in the Faraday cup is first corrected for attenuation. The resulting value is then adjusted for neutralization prior to the target cell. It is this final value that is then used in Eq. (8) as I_b in calculating the cross section. The overall correction for the worst case of 100-keV He^+ is 17%, the other beams and higher energies are less.

If the beam line prior to the collision chamber is long there also may be beam neutralization occurring as the beam traverses this distance. There is approximately 2 m of beam line from the magnet to the collision chamber at a pressure of 10^{-6} Torr. For the case of 100-keV He^+ traversing this length, assuming all the residual pressure is due to leaked target gas, we estimate that 0.06% of the beam is neutralized. This is a very small effect and we will ignore it.

One may be concerned with the results of secondary collisions within the cell. These secondary collisions could result in the neutral particle reverting back to a singly charged ion or to a doubly charged ion. Allison has examined such processes in detail [30]. For our worst case of He^+ neutralization, Allison estimates the production of He^{2+} to be less than 0.2% for energies above 50 keV. Using Allison's data for our target pressure and gas cell length, we estimate the production of neutral helium returning to singly ionized helium through a secondary collision to be less than 1%. We will ignore these effects.

III. RESULTS AND DISCUSSION

A. Carbon monoxide

Figures 1 and 2 show the spectra produced from the impact of positive ions with carbon monoxide taken in the ultraviolet and the visible wavelength regions, respectively. The ultraviolet spectrum was taken with a 300-keV He^+ beam impacting on CO, while the visible spectrum was taken with 150-keV protons.

The features that dominate the spectrum are the $B\,^2\Sigma^+ \rightarrow X\,^2\Sigma^+$ and $A\,^2\Pi^+ \rightarrow X\,^2\Sigma^+$ transitions of singly ionized carbon monoxide. The former transition, also known as the first negative band system, produces the two smaller peaks at 2190 and 2300 Å. The 2190 Å is the (0-0) vibrational transition, the 2300 Å is the (0-1) vibrational transition. The more prominent bands in the spectrum ranging form 3500 to 6000 Å are the vibrational transitions of the CO^+ $A \rightarrow X$, or comet tail, transitions.

Other characteristics of the CO^+ spectrum in this wavelength region are the $B \rightarrow A$ or Baldet-Johnson transitions. Poulizac, Desesquelles, and Dufay identify three vibrational transitions: (1-0) at 3707 Å, (0-0) at 3953 Å, and (0-1) at 4209 Å. Both Poulizac and co-workers and Aarts [31] (electron impact) report the cross sections of these peaks to be extremely small, which is confirmed here as the three peaks are virtually indistinguishable.

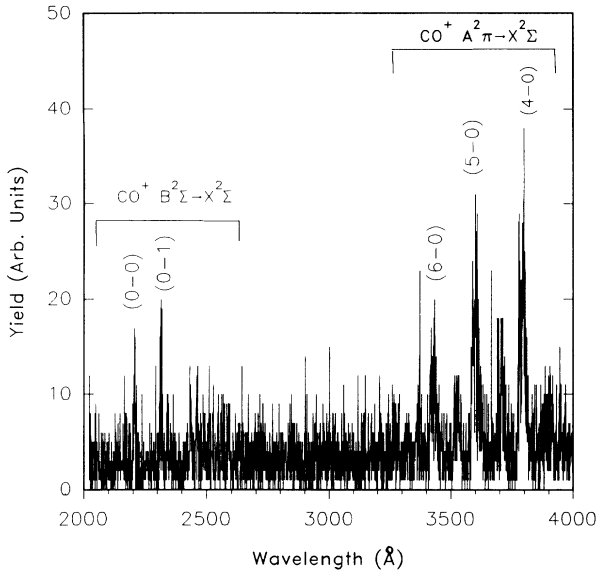

FIG. 1. Ultraviolet spectrum produced with CO as a target and a helium beam. Spectrum has not been corrected for instrument sensitivity.

Since this transition $B \rightarrow A$ would contribute to the population of the first excited state through the cascading process, the lack of photons produced from this transition would be an argument that the photon-emission cross sections produced in this investigation are actually close representations of the excitation cross section to the first excited state.

The last characteristic of the spectrum is the lines from dissociated carbon. Poulizac, Desesquelles, and Dufay identify these as C II at 2837 Å, C I at 2478 Å, C II at 4267 Å, and C 2II at 6578 Å [5]. Again, however, they are not as prominent as the CO^+ lines, indicating that ionization, not dissociation, is the primary process occurring at these energies. Also, as noted by Aarts and DeHeer [31], the overlap in the 4267-Å carbon emission and the 4260-Å (2-0) transition of CO^+ $A \rightarrow X$ is estimated to produce a 3% error in this cross-sectional measurement.

In this investigation, cross sections were taken for several of the most prominent peaks in the CO^+ $A \rightarrow X$ band, specifically, 5000 Å (1-1), 4267 Å (2-0), 4000 Å (3-0), and 3785 Å (4-0). These peaks are doublets. For 3785 Å the two peaks are distinguishable by the optical system, and the cross sections were measured with the monochromator set on each peak individually. The sum of the two measurements produced the emission cross section for the whole band. Since the dispersion of the monochromator is greater for the ultraviolet grating than for the visible grating, the doublets in the visible region were not distinguishable and were measured at one wavelength setting.

Table I lists the cross sections measured in this study, corrected for beam attenuation, as described in the experimental details. The error for each value is 20%.

Figures 3–6 show the cross sections, using CO as a target, plotted as a function of velocity. For each cross section except 5050 Å the results found here are also compared to the cross sections found by Poulizac, Desesquelles, and Dufay [5]. In general the agreement is quite good, especially when a correction factor for beam attenuation at Poulizac's lower energies is taken into account. They are, at least, certainly within Poulizac's estimation of 50% error. One more characteristic to note, however, is the absolute difference in the relationship between Poulizac's values and the values of this study for the 3785-Å line and the 4000- and 4260-Å lines.

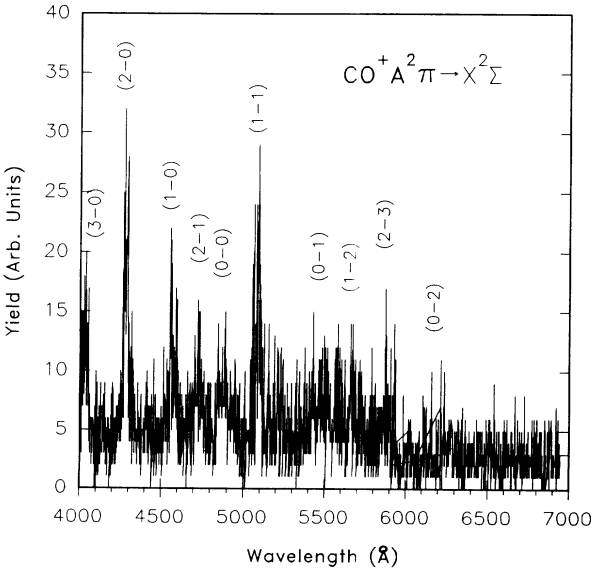

FIG. 2. Visible spectrum produced with CO as a target and a proton beam. Spectrum has not been corrected for instrument sensitivity.

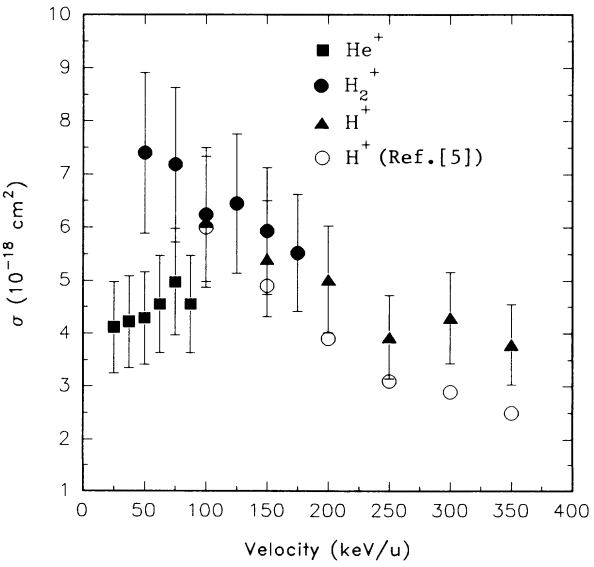

FIG. 3. Photon-emission cross sections for the 3785-Å band of CO^+ as a function of projectile velocity.

TABLE I. Photon-emission cross sections measured in this work. Cross sections are in units of 10^{-18} cm^2. Wavelength units are angstroms. Energy units are kilo-electron-volts.

		CO				CF_4					CH_4
Ion	Energy \ Wavelength	3785	4000	4260	5050	3502	3850	3901	6856	6902	4861
H^+	100	6.10	4.75	5.97	4.79						
	150	5.41	3.51	6.46	4.19						
	200	5.02	3.64	4.17	3.74						
	250	3.93	2.82	4.36	3.18						
	300	4.30	2.84	3.76	3.23						
	350	3.79	2.31	3.66	3.10						
H_2^+	100	7.40	4.94	8.24	5.15				6.54	3.36	
	150	7.18	5.10	7.58	4.77				4.57	2.83	
	200	6.24	4.83	6.85	4.33				4.50	2.54	
	250	6.45	5.05	6.30	4.19				3.88	2.33	
	300	5.93	4.85	6.04	4.16				2.57	2.16	
He^+	100	4.11	4.34	7.42	4.18	1.48	2.19	1.72	10.8	6.33	5.76
	150	4.22	4.31	7.53	4.47	2.09	3.72	2.64	11.5	7.42	5.44
	200	4.29	3.88	7.64	4.01	2.24	4.26	2.71	10.4	6.63	4.56
	250	4.55	3.68	7.11	4.19	2.31	4.59	3.14	10.9	7.03	4.49
	300	4.97	4.39	7.53	4.17	2.48	4.13	3.17	8.88	7.10	4.07
	350	4.55	4.70	7.01	4.24	2.06	3.84	2.89	7.70	6.87	3.35

Poulizac's values are higher for 4000 and 4260 Å, and lower for 3785 Å. It is possible that the dispersion used in summing the two doublets was too wide and caused an artificially high cross section, or the dispersion in the visible region was too low and not all of the peak was measured. Work done previously in this laboratory, [25] (on a different target) showed Poulizac's values to be low by a factor of 4, so a definite statement about this cannot be made.

The emission cross sections were also compared to the electron-impact emission cross sections found by Aarts and DeHeer [29]. The electron-impact cross sections were found to be significantly lower (by as much as a factor of 5 or more), although the Bethe-Born theory predicts cross sections will be only dependent on charge and velocity. The authors have no explanation for the difference, although the discrepancy has been noted by Aarts and DeHeer in their comparison with other proton-impact data.

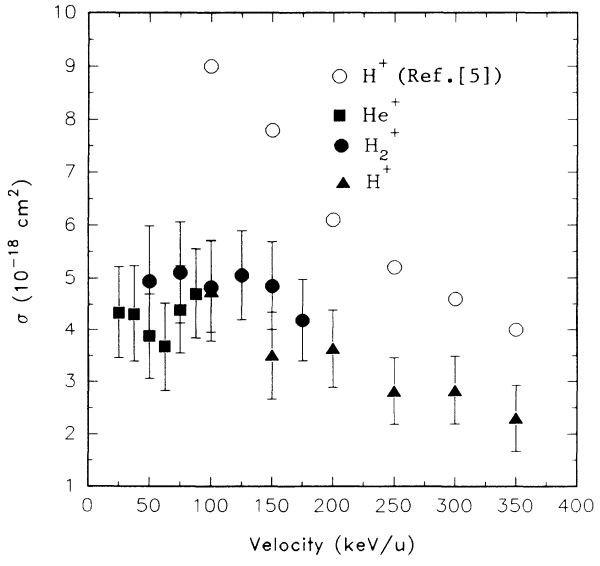

FIG. 4. Photon-emission cross sections for the 4000-Å band of CO^+ as a function of projectile velocity.

Other than the work done by Poulizac, Desesquelles, and Dufay and the electron-impact data, the authors could find no other studies of photon emission from collisions at these velocities. There are, however, several studies of charge-transfer collision processes of positive ions on CO in this energy range. Charge-transfer processes are dominated by charge capture, e.g., $H^+ + CO \rightarrow H^0 + CO^+$, or direct ionization, e.g., $He^+ + CO \rightarrow He^+ + CO^+$ with electrons released. Both of these processes contribute to the production of the first excited state of CO^+; therefore, both processes could be involved in the photon-emission cross sections examined here. By examining cross sections for these processes, the production of the A state may be better understood.

In older studies, the charge-transfer cross section and the ionization cross section could not always be directly measured by experimentalists. In some cases it is the total positive or negative charge production cross sections that are measured. With developments in the detection systems, however, as in a recent study by Shah and Gilbody [8], cross-section measurements of more specific events can be determined, such as those of dissociation and combinations of ionization and charge-transfer processes. Afrosimov *et al.* [6] could also determine the collisional processes to this extent. Figure 7 shows a comparison of the sum of the photon-emission cross sections from this work (multiplied by a factor of 30) to the direct ionization cross sections as measured by Shah and Gilbody, Afrosimov, and Rudd *et al.* One can see that the

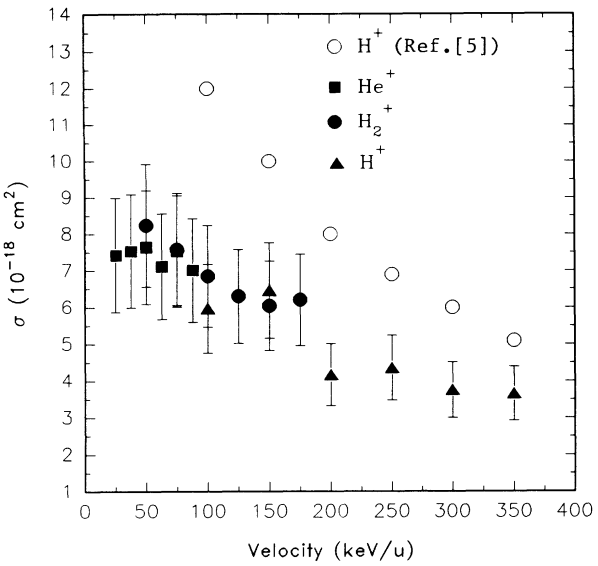

FIG. 5. Photon-emission cross sections for the 4260-Å band of CO^+ as a function of projectile velocity.

trend of the photon-emission data follows that of the direct ionization cross sections, especially with regard to a maximum at about 60 keV/u. A similar plot using the capture cross sections did not match the trend of the photon-emission data. This would suggest that the excitations measured here are a result of the CO molecule being ionized by the incoming projectile, leaving it in either the B or the A state.

This ionization process can be understood by examining the electron structure of the CO molecule. The ground-state electron configuration of CO is [32]

$$KK(\sigma_g 2_s)^2(\sigma_u 2_s)^2(\pi_u 2_p)^4(\sigma_g 2_p)^2 .$$

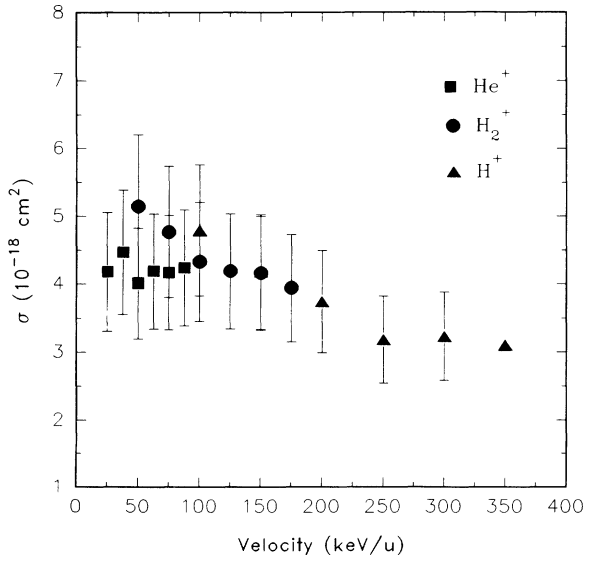

FIG. 6. Photon-emission cross sections for the 5050-Å band of CO^+ as a function of projectile velocity.

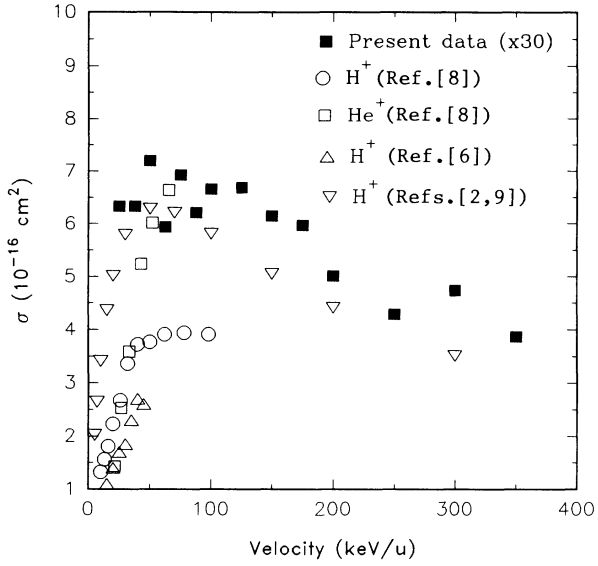

FIG. 7. Comparison of photon-emission cross sections from the present study with that of direct ionization cross sections of other workers with CO as a target.

The first excited state of CO^+ can be produced by the removal of a single π_u electron, while the B state is formed by the ionization of a σ_g valence electron.

The evidence that the excitations seen here are produced as a result of a one-step process such as direct ionization suggests the applicability of a theoretical description such as the Bethe-Born approximation. This is tested by plotting the emission cross sections on a Fano plot [33]. As can be seen in Figs. 8 and 9, the plots show a

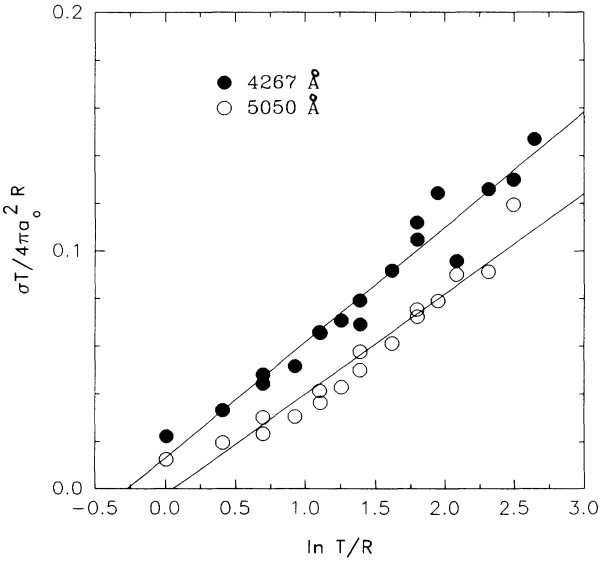

FIG. 8. Fano plot of the 4267- and 5050-Å bands of CO^+. T/R is the projectile velocity in atomic units, a_0 is the Bohr radius. Best-fit line is a linear least-squares regression at the 95% confidence level.

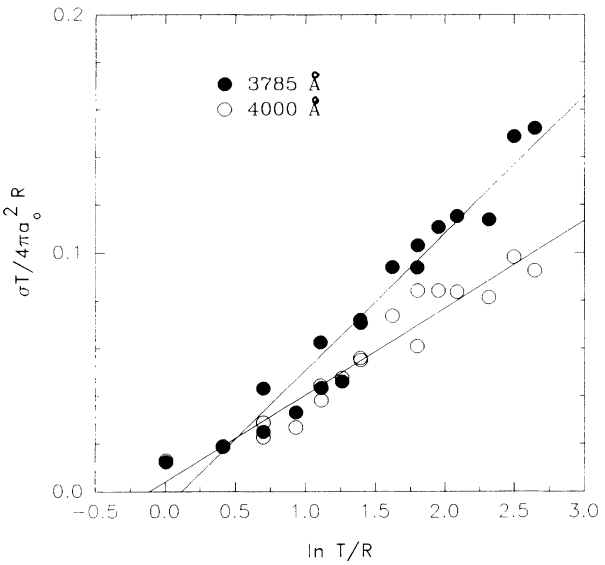

FIG. 9. Fano plot of the 4000- and 3785-Å bands of CO^+. T/R is the projectile velocity in atomic units, a_0 is the Bohr radius. Best-fit line is a linear least-squares regression at the 95% confidence level.

linear relation indicative of the reliability of the use of the Bethe-Born theory for these processes.

B. CF_4 and CH_4

The photo emission produced by using either of the two tetrahedral molecules appears to result from a more complicated process than that presented by a carbon monoxide target. Figures 10 and 11 are typical emission spectra obtained for helium impact on CF_4 and for CF_4 in the ultraviolet region. The spectrum of CH_4 is omitted as the only features present were the H_α, H_β, and He 5875-Å lines. Also, no H_2^+ or proton beam was used with the methane target, as the experimental setup did not allow separation of projectile and target emissions.

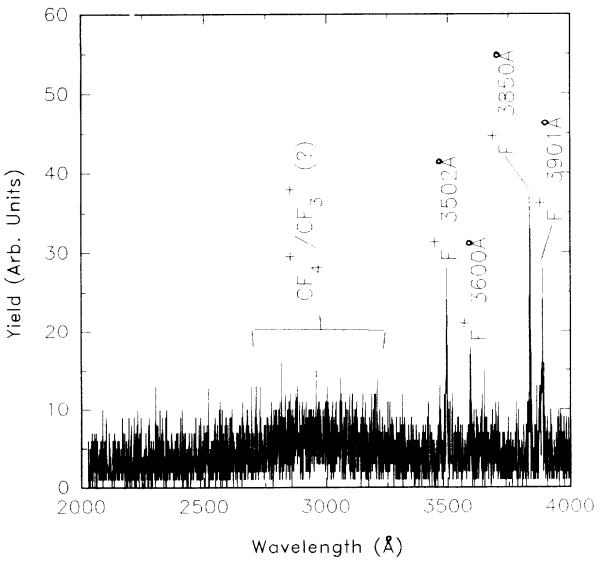

FIG. 10. Ultraviolet spectrum produced with CF_4 as a target using a helium beam. Spectrum has not been corrected for instrument sensitivity.

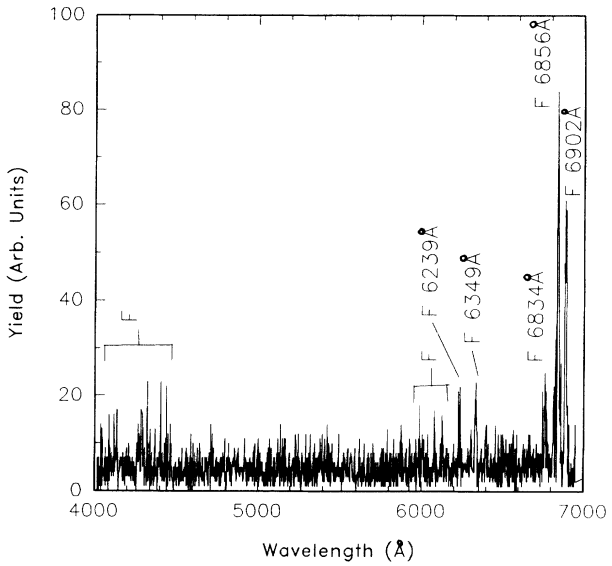

FIG. 11. Visible spectrum produced with CF_4 as a target using a helium beam. Spectrum has not been corrected for instrument sensitivity.

The broad feature in the UV spectrum of CF_4 from 2700 to 3300 Å has been identified by Aarts [21] and Van Sprang, Brongersma, and DeHeer [15] as an emission band from either CF_4^+ or CF_3^+. The remaining UV features are emissions from the F^+ fragment. The visible features are attributed mainly to neutral fluorine emission.

Although there are no other studies of ion impact spectra of CF_4 in the investigated energy region, Aarts [21]

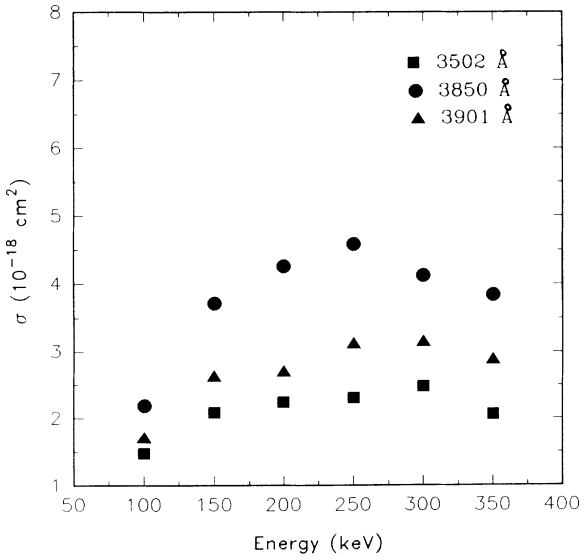

FIG. 12. Photon-emission cross sections of the 3502-, 3850-, and 3901-Å lines of F^+ from He^+ collisions with CF_4. Uncertainty in the data is 20%; errors bars are omitted for clarity.

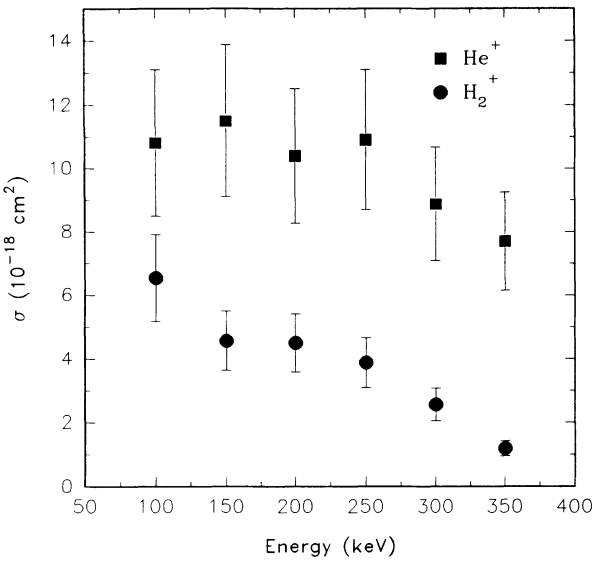

FIG. 13. Photon-emission cross sections of the 6856-Å line of F from He^+ and H_2^+ collisions with CF_4.

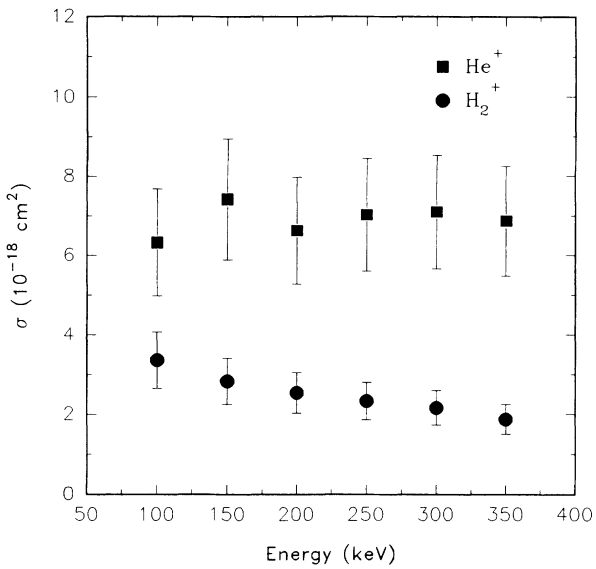

FIG. 14. Photon-emission cross sections of the 6902-Å line of F from He^+ and H_2^+ collisions with CF_4.

investigated emission from CF_4 under 1-keV He^+ impact and found no fluorine emission, but did see continuous emission bands from CF_4^+ and CF_3^+ in the region of 2000–4000 Å. The general shape of these emission bands is consistent with the present findings. Van Sprang, Brongersma, and DeHeer [15], investigating CF_4 emissions under 100-eV electron impact, saw neutral fluorine emission in the 6500–9000-Å region, as was observed in this study. Sasaki, Kuen, and Howorka [20] studied emissions from the impact of eight positive ions in the energy range of 1–1800 eV on CF_4. They found various projectile emissions in the region of 2000–6000 Å as well as F^+ and neutral carbon emission. Blanks, Tabor, and Becker [22] investigated emissions from collisions of 100-eV electrons with CF_4 and found neutral fluorine emissions in the region of 6000–8000 Å. Their spectrum is similar in feature, and also with regard to intensity ratios, to this work.

Photo-emission cross sections were measured for the 3502-, 3850-, and 3901-Å lines for He^+ impact on CF_4. The cross sections for these lines using either an H_2^+ or H^+ beam were beyond the limit of the experimental sensitivity (approximately 10^{-19} and below). For the 6856- and 6902-Å lines, cross sections for both He^+ and H_2^+ impact in the energy range of 100–350 keV were measured; cross sections using a proton beam were less than the experimental sensitivity. The cross sections of all lines at all energies investigated are given in Table I.

Figure 12 shows the cross sections for the three UV F^+ lines investigated as a function of projectile energy. The cross sections show similar dependence on projectile energy, reaching a maximum in the range of 250–300 keV. There is currently no other data available with which to compare these values.

Figures 13 and 14 show the cross sections for the two visible F lines investigated under impact of He^+ and H_2^+. The only data available for comparison at similar velocities are the 100-eV electron-impact studies of Blanks, Tabor, and Becker [22] and Van Sprang, Brongersma, and DeHeer [15]. At a velocity of approximately 170 keV/u (100-eV electrons), they report values larger than our data by a factor of 2–5.

Fano plots were made of the above data but showed no definitive linear relation. This is perhaps not surprising as the emissions seen here are from excited, dissociated atoms. The production of such fragments involves more than a simple two-body interaction, such as direct ionization, as was the situation with carbon monoxide. Thus, one would not expect the Bethe-Born theory to be a good description in this case.

IV. CONCLUSION

Photon production was examined for collisions of 100–350-keV H^+, H_2^+, and He^+ projectiles on carbon monoxide, CH_4, and CF_4.

In the case of a CO target, cross sections were measured for the (1-1), (2-0), (3-0), and (4-0) vibrational transitions for the CO^+ $A\,^2\Pi \rightarrow X\,^2\Sigma^+$ electronic transition. The measured cross sections were compared with ionization cross sections as a function of projectile energy. Based on the comparison, it appears that direct ionization of the CO target is the main contributor to the production of the excitations seen in this work. Fano plots of the photon-emission cross sections showed that the Bethe-Born theory could be applied in this case.

The excitations produced with the tetrahedral targets seem to come from a more complicated process involving dissociation than that of CO. Fano plots of this data were not conclusive.

ACKNOWLEDGMENT

This work is supported in part by a grant from the R. F. Johnson Fund from Connecticut College.

*Present address: Department of Physics, University of Connecticut, Storrs, CT 06268.
†Present address: Department of Physics, University of Arizona, Tucson, AZ 85721.

[1] R. E. Johnson, *Introduction to Atomic and Molecular Collisions* (Plenum, New York, 1982).
[2] M. E. Rudd, R. D. DuBois, L. H. Toburen, C. A. Ratcliff, and T. V. Goffe, Phys. Rev. A **28**, 3244 (1983).
[3] A. B. Pluvinal and F. Baldet, Astrophys. J. **34**, 89 (1911).
[4] J. Luu and D. C. Jewitt, Astrophys. J. **100**, 913 (1990).
[5] M. C. Poulizac, J. Desesquelles, and M. Dufay, Ann. Astrophys. **20**, 301 (1969).
[6] V. V. Afrosimov, G. A. Leiko, Yu. A. Mamaev, M. N. Panov, and M. Vuiovich, Zh. Eksp. Teor. Fiz. **65**, 495 (1973) [Sov. Phys.—JETP **38**, 243 (1974)].
[7] M. Sataka, A. Yagishita, and Y. Nakai, J. Phys. B **23**, 1225 (1990).
[8] M. B. Shah and H. B. Gilbody, J. Phys. B. **23**, 1491 (1990).
[9] M. E. Rudd, T. V. Goffe, A. Itoh, and R. D. DuBois, Phys. Rev. A **32**, 829 (1985).
[10] A. Lashof and D. R. Ahuja, Nature **344**, 529 (1990).
[11] A. Rukl, *The Astronomer's Manual* (Crescent, New York, 1988).
[12] A. Vroom, J. Chem. Phys. **50**, 573 (1969).
[13] S. Freund, S. M. Tarr, and J. A. Schiavone, J. Chem. Phys. **79**, 213 (1983).
[14] W. McLaughlin and E. C. Zipf, Chem. Phys. Lett. **55**, 62 (1978).
[15] A. Van Sprang, H. H. Brongersma, and F. J. DeHeer, Chem. Phys. **35**, 51 (1978).
[16] P. Danilevskii, I. Yu. Rapp, V. T. Koppe, and A. G. Koval, Opt. Spektrosk. **60**, 722 (1986) [Opt. Spectrosc. (USSR) **60**, 441 (1986)].
[17] W. Yates, K. H. Tan, G. M. Bancroft, and L. L. Coatsworth, J. Chem. Phys. **83**, 4906 (1985).
[18] T. A. Carlson *et al.*, J. Chem. Phys. **81**, 3828 (1984).
[19] H. F. Winters and M. Inokuti, Phys. Rev. A **25**, 1420 (1982).
[20] J. Sasaki, I. Kuen, and F. Howorka, J. Chem. Phys. **86**, 1938 (1987).
[21] J. F. M. Aarts, Chem. Phys. Lett. **114**, 114 (1985).
[22] A. Blanks, A. E. Tabor, and K. Becker, J. Chem. Phys. **86**, 4871 (1987).
[23] M. Carre and M. Dufay, C. R. Acad. Sci. **265**, 259 (1967).
[24] J. Geddes, F. B. Yousif, and H. B. Gilbody, J. Phys. B. **20**, 4773 (1987).
[25] E. L. Bryan, E. J. Freeman, and M. N. Monce, Phys. Rev. A **42**, 6423 (1990).
[26] M. N. Monce, Phys. Rev. A **37**, 3165 (1988).
[27] M. N. Monce, Phys. Rev. A **34**, 2780 (1986).
[28] E. W. Thomas, *Excitation in Heavy Particle Collisions* (Wiley-Interscience, New York, 1972).
[29] J. M. Hoffman, G. J. Lockwood, and G. H. Miller, Phys. Rev. A **11**, 841 (1975).
[30] S. K. Allison, Rev. Mod. Phys. **30**, 1137 (1958).
[31] J. F. M. Aarts and F. J. DeHeer, Physics (N. Y.) **49**, 425 (1970).
[32] G. Herzberg, *Molecular Spectra and Molecular Structure, Vol. I. Spectra of Diatomic Molecules* (Van Nostrand, New York, 1950).
[33] M. Inokuti, Rev. Mod. Phys. **43**, 297 (1971).